Environment-Related Variation in the Human Mid-Face

YAMING CUI[1]* AND SÉBASTIEN LECLERCQ[2]
[1]Key Laboratory of Vertebrate Evolution and Human Origins, Institute of Vertebrate Paleontology and Paleoanthropology, Chinese Academy of Sciences, Beijing 100044, China
[2]State Key Laboratory of Microbial Resources, Institute of Microbiology, Chinese Academy of Sciences, Beijing 100011, China

ABSTRACT

Previous studies that have examined mid-facial morphology in geographically dispersed and genetically diverse groups of humans have shown a strong adaptation of the nasal part to extreme cold environments, which was not observed in non-Arctic regions. However, it remains unclear whether different parts of the mid-face area show independent adaptation to nonpolar climates, and if so, how this adaptation impacted the morphology. To address this question, we investigated potential associations between climatic variables and the mid-facial shape in 14 populations, focusing on four aspects of the morphology: total shape, zygomatic, nasal and alveolar. The results show that when the genetic distance between populations is not considered, all aspects of the morphology are strongly correlated with all climatic variables. When the genetic distance is considered, significant correlations remain only for the zygomatic, and nasal parts with temperature, and for the nasal part and alveolar with sunshine exposure. A strong but probably artificial correlation of the alveolar with atmospheric pressure is also observed. Additionally, partial least square analyses indicate that tropical and subtropical environments are associated with smaller zygomatic and more triangular nose aperture compared to more temperate environments. These findings suggest that temperate and tropical climates have induced adaptation of zygomatic and nasal parts of the mid-face in humans, and that this adaptation was probably driven by temperature and sunlight exposure conditions. Anat Rec, 300:238–250, 2017. © 2016 Wiley Periodicals, Inc.

Key words: zygoma; function; evolution; climate; mid-face

INTRODUCTION

The diversity of human facial shapes is one of the most fascinating subjects of anthropological research. In particular, the factors that influence the morphology of the mid-face, i.e., the zygomatic, maxillary, and suborbital cavity regions, often receive high attention. It is generally accepted from earlier literature that the variance in the mid-facial morphology is associated with masticatory function in humans. Indeed, the position of the masseter muscle may play a functionally significant role in masticatory efficiency and it has been proposed that the zygomatic may be influenced by chewing movements (Hannam and Wood, 1989; Pope, 1991; Witzel and Preuschoft, 2002). However, more recent studies have seriously questioned this hypothesis. For example, the study of fifteen worldwide indigenous populations using 3-D geometric morphometric methods did not reveal any

Additional Supporting Information may be found in the online version of this article.

Grant sponsor: China Postdoctoral Science Foundation; Grant number: Grant No. 2015M581174.

*Correspondence to: Yaming Cui; E-mail: cuiyaming@ivpp.ac.cn

Received 22 February 2016; Revised 23 April 2016; Accepted 26 May 2016.

DOI 10.1002/ar.23467
Published online in Wiley Online Library (wileyonlinelibrary.com).

correlation between the masseter muscle shape and the zygomatic morphology (Noback and Harvati, 2015). In Neanderthals, the anterior teeth wear pattern relative to the posterior teeth wear pattern is less pronounced than in anatomically modern humans, suggesting that the stronger masticatory load required for raw food consumption did not influence the Neanderthal facial morphology (Clement et al., 2012). The morphological differences between Neanderthals and recent human crania may simply result from genetic drift, rather than selection driven by masticatory efficiency (Weaver et al., 2007).

As an alternative to the mastication hypothesis, recent studies have suggested that the mid-face morphology may relate to adaptation to climatic conditions. Evidence in both general and partial crania exist suggesting that climate has a significant impact on the pattern of cranial morphology (Howells, 1973; Carey and Steegmann, 1981; Howells, 1989; Powell and Neves, 1999; Harvati and Weaver, 2006; Hubbe et al., 2009; Relethford, 2009, 2010; Evteev et al., 2014). Among craniofacial regions, structures around the nose in particular have been tied to climatic factors. This observation holds even when accounting for neutral genetic distances, suggesting climatic adaptation on this part of the face (Carey and Steegmann, 1981; Roseman, 2004; Harvati and Weaver, 2006; Hubbe et al., 2009; von Cramon-Taubadel, 2009; Noback et al., 2011; Evteev et al., 2014; Noback and Harvati, 2015).

Temperature is the best-known climatic variable influencing cranial morphology. Previous studies have revealed a clear association between extreme cold and nasal structures affecting respiratory functions (Carey and Steegmann, 1981; Roseman, 2004; Roseman and Weaver, 2004; Harvati and Weaver, 2006; Holton et al., 2011; Noback et al., 2011; Holton et al., 2013; Evteev et al., 2014). However, this association was not observed in non-Arctic regions (Harvati and Weaver, 2006). Variation in nasal cavity shape follows a clinal gradient from cold-dry to hot-wet environments, and associations have been observed between the bony nasal cavity and temperature, and the nasopharynx and humidity (Noback et al., 2011). Other non-nasal regions of the face have also been associated with temperature. For example, the facial flatness and lateral expansion observed in most Asian populations have been proposed to be related to extreme cold adaptation (Coon et al., 1950; Garn, 1965), although this hypothesis was questioned in later studies (Steegmann, 1970; Shea, 1977). Pan et al. (2014) detected that the size of the zygomatic surface is significantly correlated to temperature, with populations living in colder climates showing larger zygomatics. Apart from temperature, other climatic features have also been connected to mid-facial morphology. Evteev et al. (2014) suggested that mid-facial morphology is strongly associated with winter precipitation. Noback et al. (2011) also proposed association between the morphology of the nasal cavity and precipitation. Carey and Steegmann (1981) proposed a significant negative correlation of nasal protrusion with absolute humidity, and a positive correlation with latitude.

Nonetheless, studies focusing on the correlation between climate and shapes in the non-nasal portions of the face (such as zygomatic and alveolar parts) are still sparse, and whether and how the shape of these facial parts change according to climate deserves further investigation. In addition, previous studies mostly focus on the facial measurements or geometric configurations of the facial landmarks, and the relationship between climate and the topographic characters of the mid-face has never been investigated. Finally, craniometric data has also been shown to correlate with genetic relationships between populations (Roseman, 2004; Roseman and Weaver, 2004; Hubbe et al., 2009; Relethford, 2009; Evteev et al., 2014), consistent with an isolation-by-distance model of evolutionary diversification (Hubbe et al., 2009). As climate is also tightly related to geographic distance, phylogenetic relationships, when neglected, may result in spurious correlations between facial morphology and climate variables.

Here, we investigated the correlation between various climatic parameters and the shape of zygomatic, nasal and alveolar parts of the mid-face using 3-D geometric morphometric methods, in a sample of fourteen populations of *Homo sapiens* from seven worldwide demic groups originating from different climates. As the adaptation to extreme cold has already been extensively studied and may hide more subtle relationships, populations from Arctic environments were deliberately excluded from our analysis. On the other hand, we added climatic parameters not usually investigated in previous studies, such as solar radiation and sea-level atmospheric pressure, to the more typical temperature and precipitation information in order to explore new putative associations between climate and morphology without any *a priori* hypotheses. Furthermore, we also investigated the impact of the phylogenetic relationship between populations on climate-shape correlations. Finally, we explored how the shape of the different facial parts is modified according to the climatic conditions, and discussed our results from an adaptive point of view.

SAMPLE AND METHODS

Sample

Populations. Crania were selected from osteological collections in China, Kenya, and the USA. The total cranial dataset studied comprised 112 surface scans from seven major demic groups, spanning 14 worldwide indigenous populations living in different types of climate (Table 1, Fig. 1A): Af (equatorial rainforest, fully humid), As (equatorial savannah with dry winter), Aw (equatorial savannah with dry summer), Cfa (warm temperate climate, fully humid, hot summer), Cfb (warm temperate climate, fully humid, warm summer), Cwa (warm temperate climate with dry winter and hot summer) and Dwa (snow climate with dry winter and hot summer). Only adult crania were included, and crania with obvious facial osteological deformation (e.g. alveolar atrophy) were excluded. We designed our sample to contain an approximately even distribution of males and females, since no evidence has been found indicating gender bias in the climatic impact on facial morphology.

The selected crania were subsequently scanned with a Konica Minolta noncontact three-dimensional (3-D) digitizer Range 7. The resolution of the surface scanner is 40 μm. All scans were reconstructed to a 3-D mesh with the software Rapidform VOX 2® (INUS Technology).

TABLE 1. Overview of morphological sample, including the number of individuals per population, the matched genetic populations, the longitudes and latitudes, and the values of the climatic variables

Location	Province	N	Genetic samples	Latitude	Longitude	T_{max}	T_{min}	S_{max}	S_{min}	P_{max}	P_{min}	S_{max}	S_{min}
Chinese North	Jilin	6	CHB	43.86847	125.3147	11	−0.36	714.72	238.78	181.505	4.80256	1027.96	1004.94
	Shandong	5	CHB	36.66853	117.0204	19.81	9.87	761.61	343.43	187.138	5.97297	1027.95	1005.08
	Hebei	8	CHB	38.03706	114.4687	19.09	7.77	745.7	361.03	160.366	3.35	1031.2	1003.8
Chinese South	Jiangxi	8	CHS	28.71376	115.8529	21.86	14.74	628.85	268.4	259.414	50.1645	1026.22	1004.01
	Yunnan	7	CHS	24.95324	102.7376	21.01	10.6	716.95	449.86	207.337	11.9202	1016.88	998.477
	Guizhou	8	CHS	26.64766	106.6302	19.96	11.96	520.88	189.56	215.03	23.6357	1026.79	1003.49
	Guangxi	6	CHS	25.27357	110.2902	23.21	15.7	576.69	222.82	341.742	46.3055	1021.56	1003.66
Southeast Asian	West Java	8	JAV	−6.20876	106.8456	32.02	24.12	795.94	555.93	345.124	50.106	1010.47	1009.53
	East Java	6	JAV	−7.077	113.2822	32.12	24.23	839.17	660.17	334.159	49.881	1011.39	1009.07
Australian aboriginal	Darwin	13	MEL	−12.4628	130.8418	32.02	23.19	844.78	647.04	403.689	0.66	1013.08	1006.28
European	Germany	13	GBR	52.52001	13.40495	14.12	6.15	582.97	124.71	66.8187	34.0635	1016.67	1014.07
	Austria	12	GBR	47.51623	14.55007	13.99	6.36	533.22	187.11	140.92	55.0556	1020.92	1013.96
American Indians	Florida	16	MEL	28.26393	−80.7214	25.85	19.43	778.18	441.68	189.395	39.7048	1020.53	1015.84
East African	Kenya	18	LWK	−1.29207	36.82195	23.46	20.2	766.01	470.65	233.244	17.873	1014.24	1008.74

Shape Data

The landmarks and semilandmarks were designed to best reflect the mid-facial shape. The total mid-facial dataset was divided into three parts: (1) The zygomatic dataset (eight landmarks, fourteen curve semilandmarks, and 177 surface semilandmarks) represents the overall shape of the zygomatic bone; (2) the nasal dataset (four landmarks, 26 curve semilandmarks, and 180 surface semilandmarks) represents the shapes around the nasal aperture, the topography of infraorbital surface; (3) the alveolar dataset (three landmarks, 21 curve semilandmarks, and 96 surface semilandmarks), represents the prognagm and alveolar morphology (Fig. 2).The zygomatic and nasal parts are separated based on the zygomaticomaxillare suture, reflecting the morphology of the nasal and cheek area, respectively, while the alveolar process of the maxilla is considered to be alveolar. The four datasets (total, zygomatic, nasal, and alveolar) were analysed separately in all subsequent procedures.

Landmarks were chosen on each individual so as to be homologous across all specimens, as suggested by Martin (1988), and their 3-D coordinates were acquired (Table 2). Sliding curve semilandmarks were digitized along the major curves of the vault, including the curves of the sagittal, occipital and brow ridges, and each was manually re-sampled on each individual specimen. The landmarks and curve semilandmarks on all specimens were digitized by one author (Y. C.). The surface semilandmarks were digitized according to the techniques described by (Freidline et al., 2012a,b, 2013, 2015).

First, a mesh of surface semilandmarks was digitized using one of the specimens in this study as a 'template' individual. This mesh of surface-semilandmarks was then warped into the vicinity of the surface of every specimen with a thin-plate spline (TPS) interpolation (Bookstein, 1989; Gunz et al., 2009a,b; Freidline et al., 2012a,b, 2013, 2015). The warped points were later projected on to the surfaces by picking the closest vertices from the original surface point clouds of the specimens, following protocols described in previous studies (e.g., Gunz, 2005; Gunz and Harvati, 2007; Gunz et al., 2009a; Harvati et al., 2010; Freidline et al., 2012a,b, 2013, 2015). This procedure produce the same number of surface semilandmarks as the template by downsampling the scanned mesh and registering the template with the current specimen via generalized procrustes analysis (GPA). A nearest neighbour algorithm was used to match the template surface landmarks to the surface of the current specimen. This protocol ensured that every specimen had exactly the same number of surface-semilandmarks, and that the surface-semilandmarks of every specimen were located approximately in corresponding positions, as required in geometric morphometrics. To remove the effect of arbitrary positioning of the surface semilandmarks, they were slid along planes tangent to the surface, minimizing the TPS bending energy between each specimen and the Procrustes mean shape. These procedures were performed based on protocols established in previous studies (Gunz, 2005; Gunz et al., 2009b; Freidline et al., 2012a,b, 2013, 2015).

To ensure that the later analyses focused only on the shape differences between specimens and not on the variation in size or on the orientation of the landmark

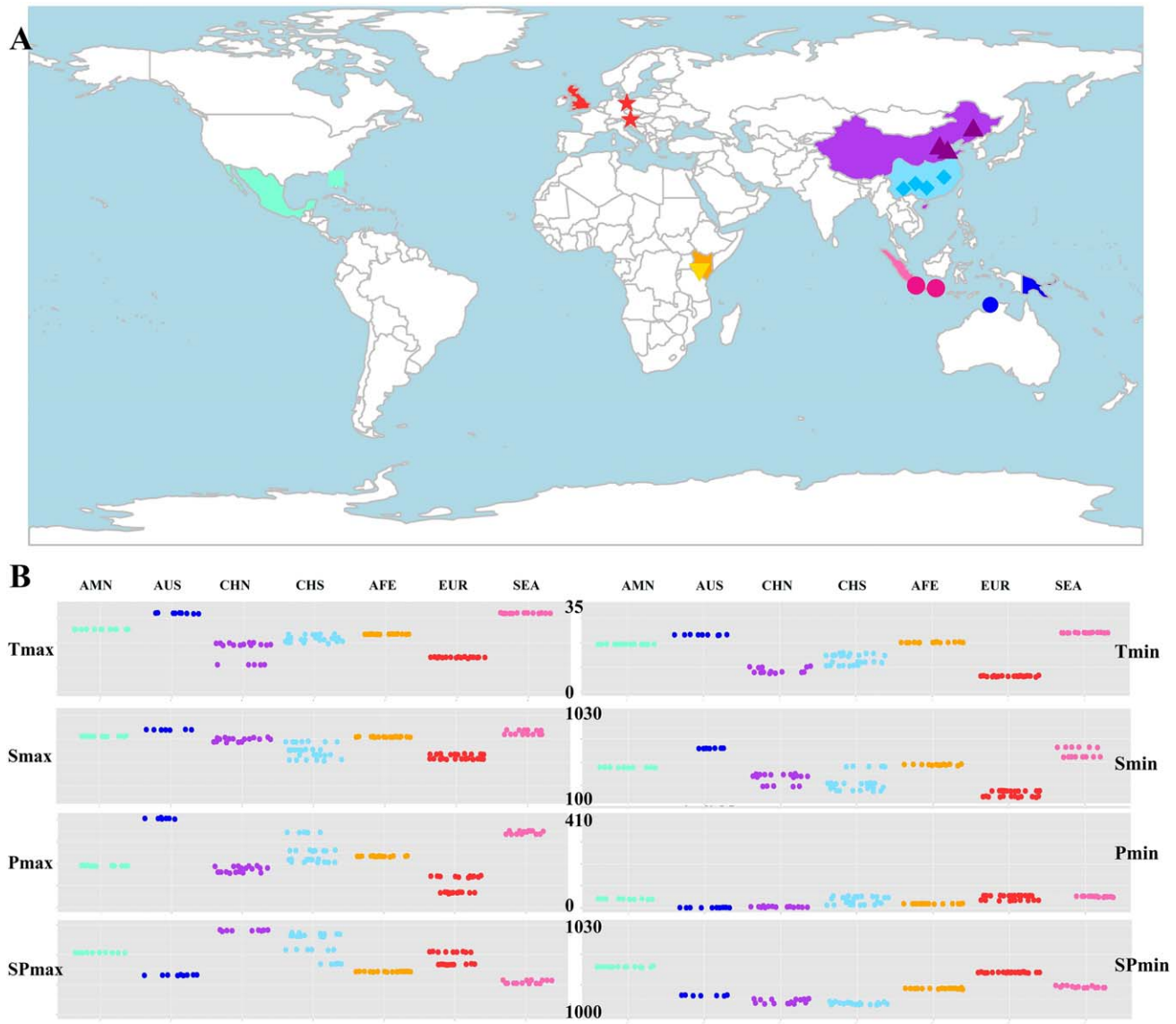

Fig. 1. (A) Genetic and morphological modern human population samples employed in this study, the dots indicate morphological populations, the colored geographic areas indicate genetic populations; (B) Jitter plots indicates the values of the climatic variables included in this study.

configurations, all landmark and surface-semilandmark coordinates were processed using GPA. GPA superimposes multiple landmark configurations by translating them to a common origin, scaling them to unify centroid sizes, and rotating them into a uniform orientation according to a least-squares criterion. All data processing and subsequent statistical analyses were performed using R (R_Developmen_Core_Team, 2013) and the Geomorph R package (Adams and Otarola-Castillo, 2013).

Climate Data

The climatic data were obtained from the KNMI Climate Explorer database (http://www.climexp.knmi.nl) on 23 October 2015 for the sampling locations included in this study (Table 1). We used the mean temperature of the warmest and coldest month (°C, T_{max} and T_{min}), the mean precipitation of the wettest and driest month (mm, P_{max} and P_{min}), the highest and lowest monthly sea level pressure (mb, SP_{max} and SP_{min}) and the highest and lowest monthly surface solar radiation (S_{max} and S_{min}) as climatic indicators for each population. These indicators are listed in Table 1 and visualized in Fig. 1B. The temperature, precipitation and sea level pressure data was retrieved from the monthly station data (for the exact period see Supporting Information Table S1) in the KNMI dataset, and surface solar radiation data was obtained from the FRESCO dataset at 0.5°C, for the years 2002–2012.

To meet the requirements of the statistical package for the Mantel and partial Mantel tests (see below), the variables belonging to the same categories were

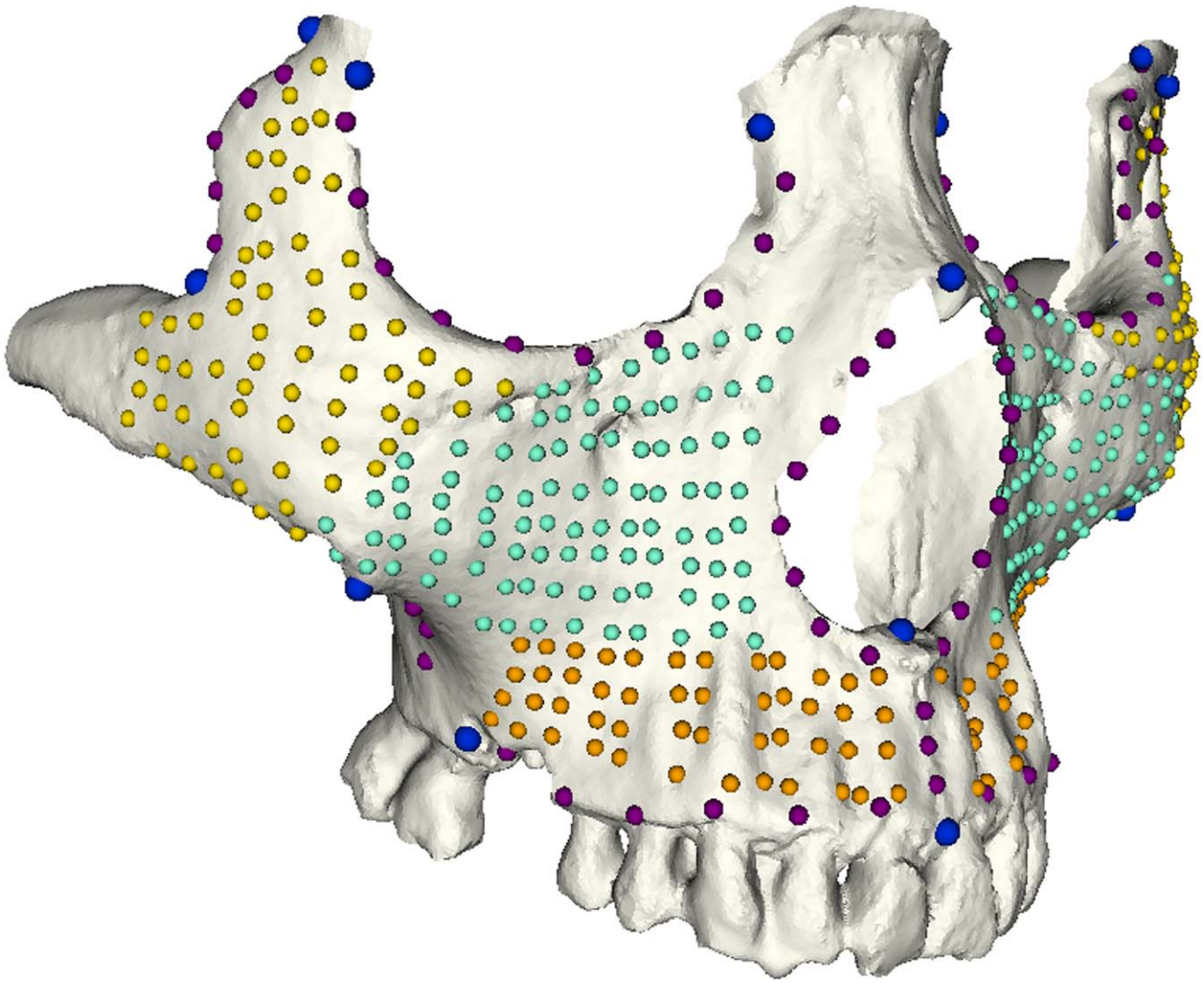

Fig. 2. Landmarks (blue), curve-semilandmarks (purple), surface-semilandmarks (yellow for the zygomatic dataset, light green for the nasal dataset, and orange for the alveolar dataset) used in the analysis.

combined into a single variable in the matrix: temperature (T, including T_{max} and T_{min}), precipitation (P, including P_{max} and P_{min}), sea level pressure (SP, including SP_{max} and SP_{min}) and solar radiation (S, including S_{max} and S_{min})

Genetic Data

Genetic information was collected from the 1000 Genomes Project (The 1000 Genomes Project et al., 2012) and the PanAsian SNP project (PanAsian SNP Consortium et al., 2009). Exact matching of morphological samples with genetic samples is not possible due to limitations in both data sets. Matching between geographic neighbors was therefore conducted in order to preserve a meaningful number of samples (e.g., Harvati and Weaver, 2006). Genetic samples from the British (GBR, 107 individuals), Kenyan (LWK, 116 individuals), Han Chinese from Beijing (CHB, 108 individuals), Southern Han Chinese (CHS, 171 individuals) and Mexican descendants from Los Angeles (MXL, 107 individuals) were selected in the 1000 Genomes Project dataset to represent German/Austrian, Kenyan, Han North, Han South, and American Indian populations, respectively. Javanese (JA + JV, 53 individuals) and Melanesian (MEL, 5 individuals) genetic samples were selected from the PanAsian SNP project to represent Indonesian and Australian populations, respectively. The geographic distance between the matched genetic and morphological samples was greatest in two cases: the Australian samples and the American Indian samples. However, for each of these groups, the genetic and morphological populations share recent population history and are from similar latitudes and climatic conditions. It is important to point out that any error introduced by this imperfect matching of samples will bias the results towards not finding significant associations between morphology and genetic background (Roseman, 2004; Harvati and Weaver, 2006).

The genetic information consisted of a list of SNPs (single nucleotide polymorphisms, i.e., a genomic location that shows nucleotide variation in a population) for each chromosome. SNPs were retrieved from chromosomes 10,

TABLE 2. Landmarks and curve semilandmarks used in the analyses

Landmark	Abbreviation	Description
1. Rhino	Rhi	
2. Nasospine	Ns	
3. Prosthion	Pr	
4,5. Frontomalare orbitale	Fmo	
6,7. Maxillofrontale	Mf	
8,9. Zygomaxillare	Zm	
10,11. Frontomalare temporale	Fmt	
12,13. Jugale	Ju	
14,15. Inferior root of zygomatic process	Zri	Position of malar root of arch projected onto buccal alveolar surface, following Freidline (2012b)
Curves		Description
1. Lower orbital margins		Right and left, $N = 10$.
2. Nasal aperture margin		$N = 16$
3. Nasospine to prosthion		From nasospine to prosthion, along the midsagittal plane. $N = 3$
3. Alveolar margin		From prosthion to inferior root of zygomatic process, along the alveolar margin. Right and left, $N = 6$
4. Lower margin of zygomatic body		From zygomaxillare to inferior root of zygomatic process, along the lower margin of zygomatic bodies. Right and left, $N = 3$
5. Posterior margin of frontal processes of zygomatic bones		From frontomalare temporale to jugale, along the posterior margin of frontal processes of zygomatic bones. Right and left, $N = 5$

21, and 22, which resulted in 2821, 969, and 313 SNPs common to both databases, respectively. No further information was retrieved from other chromosomes, because the above three chromosomes returned exactly the same results in the Mantel and partial Mantel tests (see below). The frequency of each nucleotide (A, T, G or C) at each SNP was then calculated for each population and stored in a three dimensional matrix with axes of SNP, Population and Nucleotide Frequency. Between-population distances were computed from this dataset using the same methods applied to the morphological data, by considering each SNP position as a landmark and each nucleotide frequency as a coordinate.

Statistical Methods

Test for climate-shape correlations. To test for correlations between mid-facial shape, climate and genetic data, we used Mantel matrix correlation tests (Mantel, 1967) in ecodist (Bjornstad and Falck, 2001), an R function package. Euclidean distances were calculated between each specimen for climate and genetic data, and Procrustes distances for shape data were used as inputs in Mantel tests. Matrix permutations (10,000 iterations) were then used to assess significance, with the alpha level set at $\alpha = 0.05$.

To account for population history effects, we ran partial Mantel tests on the correlation between cranial shape and climate in which matrices of genetic distance between populations (as a proxy for population history, following Evteev et al., 2014; Noback and Harvati, 2015) were kept constant. For the partial Mantel tests, a Holm-Bonferroni correction was also applied to correct for multiple comparisons (Holm, 1979). Permutations (10,000 iterations) were then used to calculate significance, with the alpha level set at $\alpha = 0.0167$.

Visualizing climate-related cranial shape. To explore and visualize specific shape changes related to climate, we performed two block partial least squares (2B PLS) analyses (Rohlf and Corti, 2000). This is a very powerful and generalized approach for ordination and statistical hypothesis testing, and allows users to test hypotheses about the inter-relations between blocks of observations made on the same objects. The first block of data consisted of the Procrustes coordinates for mid-facial shape; the second block comprised climate variables (Table 1). The 2B PLS analysis calculates new pairs of variables, one for the shape (singular warp) and one for climate (latent variable) that best explain the covariance between the two blocks. This analysis allows associations among morphological and climate blocks of data to be related to specific morphological and climatic variables. Loadings were summarized in bar charts to facilitate interpretation. The strength of the covariation is represented by the RV coefficient and the shape change related to this covariance can be visualized (Noback et al., 2011; Noback and Harvati, 2015).

RESULTS

Climate-Facial Shape Correlations

We first explored putative correlations between the total shape of the mid-face and a set of climatic variables: temperature, sunshine exposure, precipitation level and sea-level pressure. Our Mantel tests returned very significant correlations for all the climatic variables, although the correlation coefficient was low ($r < 0.17$ and $P < 0.01$ in all cases; Table 3). However, when partial Mantel tests were used to correct for the genetic distance between populations, all the correlations became nonsignificant ($r \leq 0.07$, $p > 0.05$; Table 3). This suggests that the global mid-facial morphology is mainly driven by the genetic relatedness between populations rather than by climatic conditions.

Considering the zygomatic, nasal, and alveolar parts of the mid-face independently provided similar results with the Mantel test: the shape of all three subsets is

TABLE 3. Mantel and partial Mantel test results for the association of morphological distances with climatic distances

Climatic parameters	Total				Zygomatic				Nasal				Alveolar			
	Original		Corrected		Original		Corrected		Original		Corrected		Original		Corrected	
	Corr.	*P* value	Corr.	*P* value	Corr.	*P* value	Corr.	*P* value	Corr.	*P* value	Corr.	*P* value	Corr.	*P* value	Corr.	*P* value
T	**0.1697**	0.0001	0.07047	0.0554	**0.1904**	0.0001	**0.1131**	0.0058	**0.2312**	0.0001	**0.1018**	0.0148	**0.1283**	0.0007	0.0841	0.035
S	**0.0958**	0.0009	0.007802	0.782	**0.1062**	0.0008	0.0362	0.226	**0.2090**	0.0007	**0.0914**	0.0118	**0.1342**	0.0003	**0.0947**	0.0067
P	**0.0956**	0.0096	−0.01148	0.779	**0.0967**	0.0126	0.0111	0.7949	**0.2070**	0.0111	0.0537	0.2544	**0.1578**	0.0111	0.1100	0.0196
SP	**0.1545**	0.0001	−0.01432	0.726	**0.0976**	0.0007	−0.0463	0.2975	**0.1051**	0.0007	−0.0519	0.2473	**0.2531**	0.0001	**0.2206**	0.0001

Bold values indicate significance value (Mantel tests at $P < 0.05$, partial Mantel tests at $P < 0.016$).

very significantly correlated with all the climatic variables included in this study (Table 3). After correction however, some significant correlations remain: the zygomatic shape with temperature, the nasal shape with temperature and solar radiation, and the alveolar shape with solar radiation and sea-level pressure (Table 3). The strongest correlations exist between the zygomatic and temperature ($r = 0.113$, $p = 0.0058$), and the alveolar and sea-level pressure ($r = 0.221$, $P < 0.0001$). Different climatic conditions thus seems to impact the shape of various parts of the mid-face independently, with temperature, and sunshine having a moderate general effect, and pressure having a higher and more specific effect on the alveolar section.

Our dataset includes samples from an American Indian population, which are known to retain morphological traits from their Siberian ancestors despite living in a much warmer climate. To explore the putative effect of this population on our observations, we conducted a new correlation analysis with the American Indian population excluded from the dataset. The results show only minor variations compared to the study with all populations: the uncorrected correlation between zygomatic and climatic variables precipitation and pressure became nonsignificant, as well as the corrected correlation between alveolar and sunshine; the value of the corrected correlation between the nasal part and temperature also slightly increased (Supporting Information Table S2). The absence of any difference between the two datasets suggests that the American Indian population has sufficiently differentiated from their Siberian ancestor such that the correlation between climate and mid-face morphology was not blurred. We therefore kept the complete dataset in the following analyses, to retain native populations representative of all continents.

Visualizing Climate-Related Mid-Facial Shape

We next investigated the proportion of inter-individual morphological variation explained by climatic variables using a PLS analysis. Overall, the climatic parameters selected here account for 28.51% of the mid-facial shape total variance. The first two PLS dimensions together explain 92.28% of the total covariance of the morphological and climatic blocks (PLS1: 73.37%, PLS2: 18.91%).

The first pair of singular vectors (SV1) shows a very strong correlation coefficient between shape and climate ($r = 0.629$, $P < 0.0001$) and essentially reflects a gradient from temperate to tropical climates, including East and West Java, Australia and East Africa (Fig. 3A). The loadings of the climate variables indicate that the climate-shape correlation in SV1 is positively influenced by temperature, sunshine, and maximal precipitation level, and negatively influenced by the minimal precipitation level and maximal atmospheric pressure (Fig. 3B). According to the loadings of the morphological variables (Fig. 4), the tropical climate is associated in the zygomatic portion with a more anteriorly placed processus frontosphenoidalis; more anteriorly and posteriorly positioned zygomatic arches, both of which are less flared; a higher and more forward protruding inferior orbital margin; and a less robust and more superiorly posited zygomatic tubercle. In the nasal portion, it is associated with a shorter and narrower frontal process

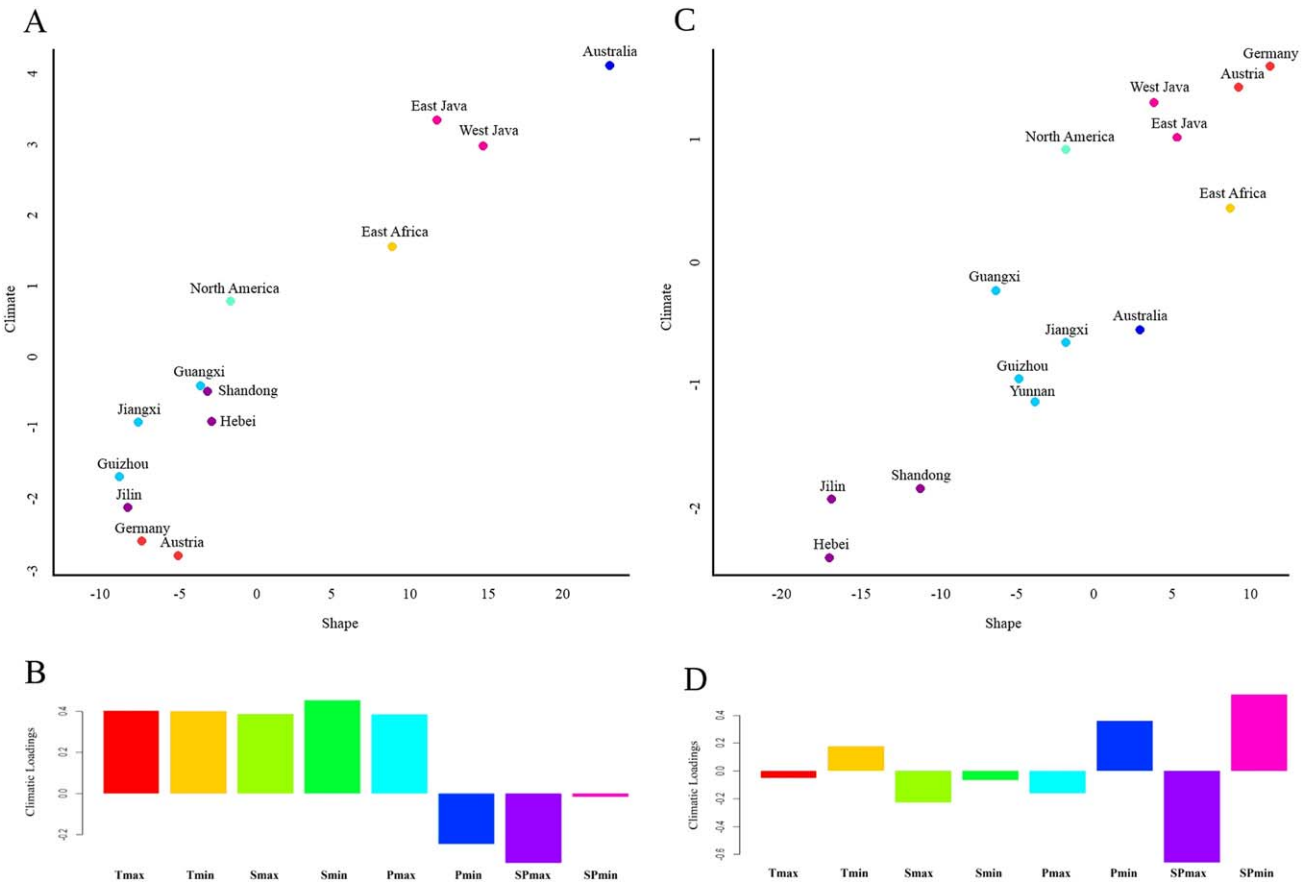

Fig. 3. Scatter plot of mid-facial and climate variables. (A, C) Plots of the first and second singular vectors from PLS. (B) Plot of the second singular vectors from PLS. Colors indicate genetic groupings. (B, D) Loadings of variables on the first and second singular vectors of the climatic variables, respectively.

of maxilla; a more laterally expanding maxilla; a less marked canine fossa; and narrower/wider nasal aperture upper/lower regions, respectively. Finally, in the alveolar portion, it is associated only with an anteriorly and inferiorly protrusive alveolar process. In summary, populations from tropical climates show a less pronounced zygomatic bone and a wider but lower nasal aperture than populations living in more temperate climates.

In the second pair of singular vectors (SV2), shape and climate are also clearly correlated ($r = 0.565$, $P < 0.0001$, Fig. 3C). Contrary to the correlation in SV1, the most important explanatory climatic variable in SV2 is atmospheric pressure level. The correlation is positively influenced by the minimal atmospheric pressure level and very negatively influenced by the maximal atmospheric pressure level (Fig. 3D). In comparison, temperature and sunshine variables appear to have little effect on the climate-shape correlation in SV2. The minimum precipitation level also has a moderate positive influence on the correlation, but not to the same degree as for the maximum precipitation level. The SV2 correlation thus reflects a gradient between populations originating from regions with high annual variation in atmospheric pressure level and populations originating from regions with a more constant annual pressure level. The loadings of the shape variables in SV2 show that higher pressure variation is associated with a less laterally expanding mid-face, a less laterally and superiorly expanded processus frontosphenoidalis, a more inferiorly placed zygomatic portion, and more robust zygomatic tubercles; the inferior portion of the nasal aperture expands laterally but the superior portion is narrow, with a higher nasal aperture height; more posteriorly protruding aperture and alveolar process, alveolus is less expanded along mid-sagittal and coronal plane, alveolar height is lower.

DISCUSSION

In this study, we found that several climate parameters are significantly correlated with the shape of the mid-face. Some parameters, like temperature and sunshine, are moderately associated with different subregions of the mid-face, while others, like atmospheric pressure, show a more pronounced association with only a single subregion (the alveolar part in this case). This indicates that several environmental forces may impact the morphology of the cranium independently.

According to our observations, the strongest effect is connected to a gradient from temperate to tropical climates, and mostly affects the zygomatic and nasal aperture shapes. This agrees with the suggestion from Harvati and Weaver (2006), which implied that non-

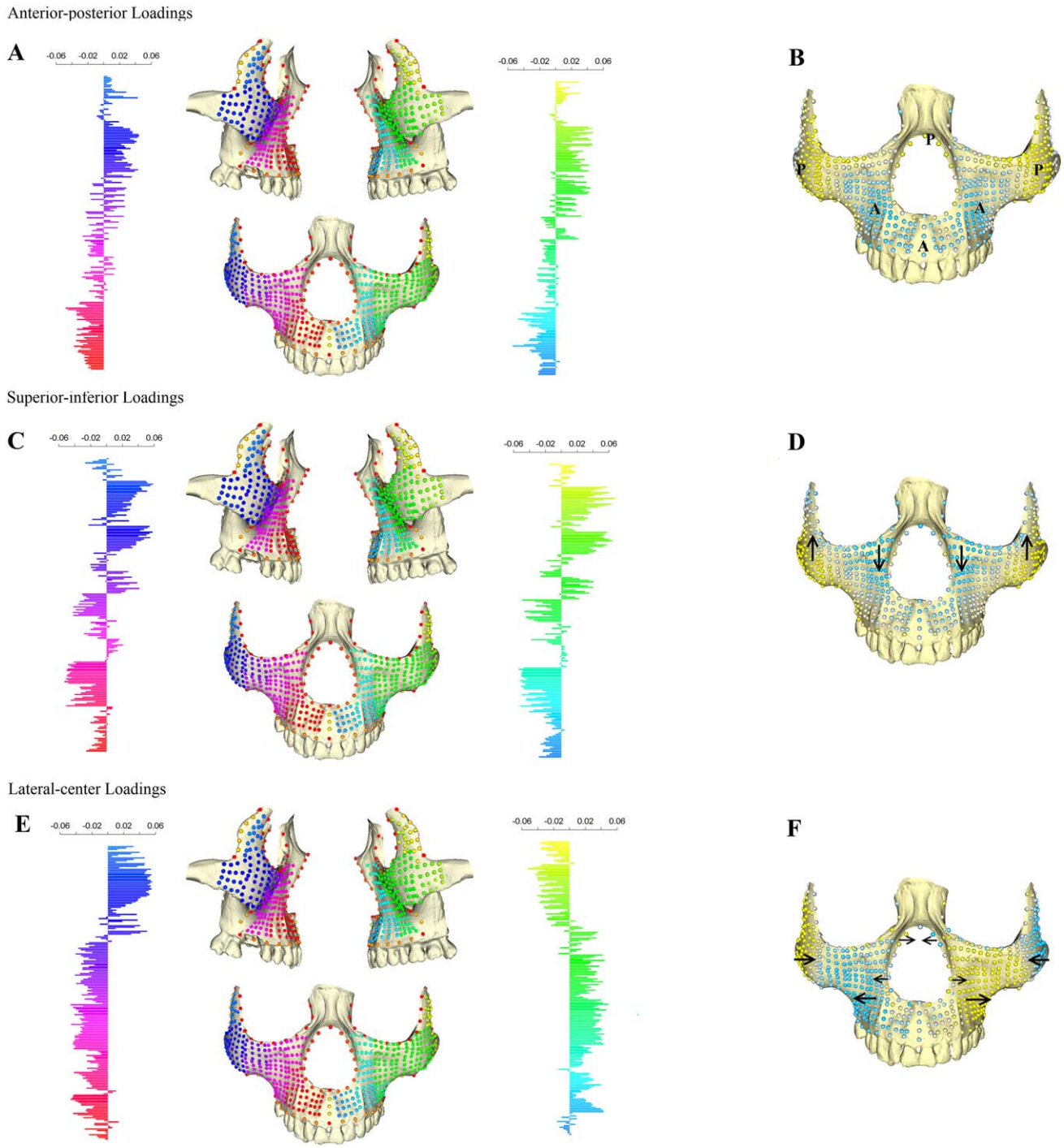

Fig. 4. Morphological loadings of the climatic variables along the first singular vectors from PLS. The bar charts in figures (A, C, E) illustrate loadings of variables on the first singular vectors of the morphological variables along with mid-facial shape with gradient colors marking the corresponding facial portions; (B, D, F) indicate the loading values on each landmark and semilandmark along the three orthogonal directions.

nasal aspects of the face may be associated with climate, especially in the zygomatic region. Why their study fails to confirm the association while ours succeeded is possibly due to different sampling protocols. Although 3-D geometric morphometric methods were also employed by (Harvati and Weaver, 2006), they limited their analysis to osteometric landmarks, which emphasizes the geometric relationships among landmarks. Our use of surface semilandmarks provides a more complete estimation of the topology of the mid-face surface, which may have

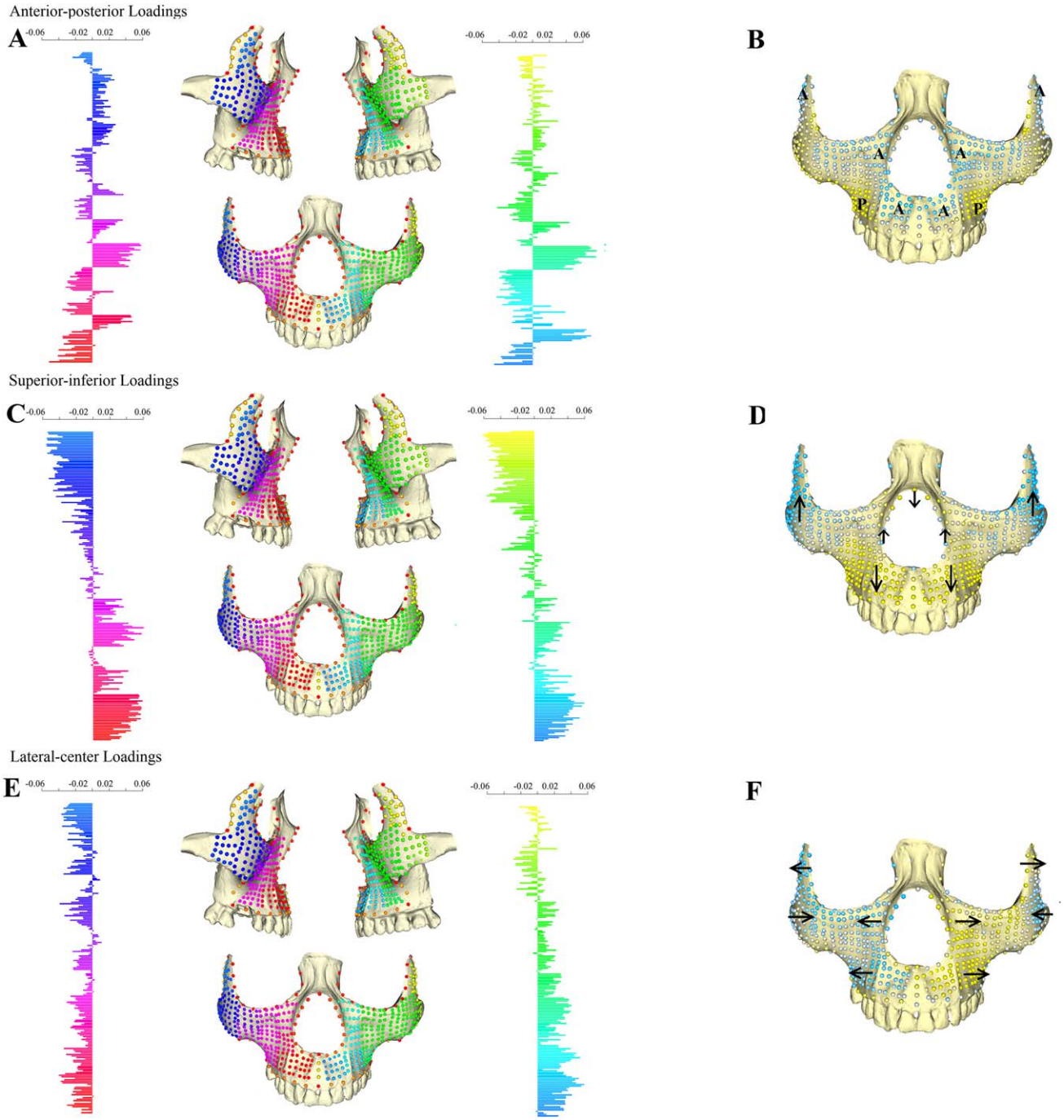

Fig. 5. Morphological loadings of the climatic variables along the second singular vectors from PLS. The bar charts in figures (A, C, E) illustrate loadings of variables on the second singular vectors of the morphological variables along with mid-facial shape with gradient colors marking the corresponding facial portions. (B, D, F) indicate the loading values on each landmark and semilandmark along the three orthogonal directions.

provided sufficient data to observe a significant correlation. On the other hand, the use of a large number of surface semilandmarks may have introduced greater variation, which may explain why our correlation coefficients are lower than in other studies exploring associations between mid-facial morphology and climate using linear measurements or osteometric landmarks (Harvati and Weaver, 2006; Noback et al., 2011). Another possibility is that only a small part of the morphological variation can be explained by climatic differences. Our results also show that the methodology is robust with regard to the inclusion of confounding populations, such as those

showing remnants of ancestral morphological features linked with very different climates.

The influence of population history on human cranium morphology have long been recognized but cannot fully explain differences between populations, especially regarding the mid-facial region of the skull (Smith, 2011; Evteev and Movsesian, 2016). In the present study, all the correlations between climatic variables and the total facial morphology disappeared when genetic distance was taken into account, indicating that these correlations were driven by the nonadaptive part of the shape variation. Consequently, the correlations that remained for mid-face subparts after genetic distance correction can be more confidently attributed to some kind of geographical adaptation unrelated to population history. Evteev and Movsesian (2016) suggested that the use of multiple neutral population distance markers (i.e., mtDNA, SNPs, and cranial nonmetrics markers) should be considered when exploring the association between face morphology and climatic factors, to avoid the specific drawbacks of each type of data. According to the same authors, SNPs are the technically most reliable markers, but they suffer from small sample sizes and from insufficient representation of populations at the local scale. However, our analysis are not affected by these limitations, since our morphological samples are differentiated at the global (worldwide) scale with corresponding genetic samples available in the 1000 Genomes Project and the PanAsian SNP databases, and since almost all the selected genetic populations included more than 50 individuals.

One important issue concerning results involving an association between temperature and both zygomatic and nasal portions of the facial shape is whether the observed temperature–zygomatic shape association is due to adaptation to clinal temperature or is simply a side effect of the shape differences around the nasal aperture. Indeed, possible morphological integration between nasal and non-nasal parts of the face have been previously proposed (Ackermann, 2005). The present analysis shows that the zygomatic and nasal regions are both significantly correlated with temperature when tested separately in the partial Mantel tests. However, no significant correlation was detected between the total mid-facial morphology and temperature, suggesting that the zygomatic and nasal portions do not always change in accordance. Therefore, we tentatively conclude that the association between climate and the zygomatic more likely reflects an independent response of the zygomatic to climate rather than integration between the nasal and zygomatic areas.

Morphologically speaking, our results show that the zygomatic tubercle is less robust, that the zygomatic arches are less flared, and that the positions of the zygomatic body and zygomatic arch are more angular in temperate climate populations than in tropical climate populations. Overall, these differences lead to a wider zygomatic eminence in populations living in more temperate climates. These observations are in agreement with a previous study reporting a negative correlation between zygomatic surface and annual temperature average (Pan et al. 2014). Although the authors of this study suggested that such correlation was driven by nonadaptive forces (genetic drift, by-product of the braincase shape), a biological explanation can be put forward. The zygomatic bony structure is the fixation point for the zygomatic ligament, which itself supports the cheek's fat compartments (Rohrich and Pessa, 2007; Rossell-Perry, 2013). Body fat plays a critical role in temperature regulation, and the extra fat induced by larger zygomatic arches may substantially reduce heat loss in climates with cooler temperatures. This hypothesis is supported by the observation that ~25% of total body heat loss come from the head and face (Beall et al., 2012). Since the face, especially the cheeks region, is the only body part usually not protected by hair or clothes, zygomatic shape adaptation allowing better temperature regulation may be expected.

It has been suggested that the nasal aperture becomes narrower relative to its height in Arctic populations compared to temperate environment inhabitants, likely due to an increase in air mixing and a decrease in the airstream velocity (Evteev et al., 2014). We also observed these features related to cold adaptation in populations from temperate climates. We show that the width of the nasal aperture in different populations follows a gradient pattern from temperate to tropical climates, with a wider aperture in tropical regions and a narrower aperture in temperate regions. In addition, our study reveals that the positive association between aperture width and climate is only present in the inferior portion of the aperture, while the superior portion shows a negative association. The entire aperture shape thus resembles a triangular shape in tropical regions and a rectangular shape in temperate regions. The enlargement of the inferior portion of the aperture also reverberates on the alveolar bone in the vicinity of the nasal part, leading to a wider alveolar in populations from tropical climates. Strikingly, the morphology of these two mid-face regions (nasal part and alveolar) is correlated with sunshine exposure variation, suggesting that the triangular shape for the nose is linked to this climatic factor. The nose is the region the most exposed to sunlight radiation in the human face, and is subject to high incidence of basal cell carcinoma (Airey et al., 1995; Downs and Parisi, 2009), though its impact on selection is under debate, due to its late occurance in life (Blum 1961; Jablonski and Chaplin, 2000). In tropical regions, where the sunshine exposure is high, the triangular nose aperture shape may thus lead to a less prominent nose, reducing the probability of cancer development. Flattened nose individuals may also be less subject to sunburns, providing an additional selective advantage for this kind of nose shape in tropical climates compared to temperate climates.

We also detected previously not described aspects of mid-facial morphology that are associated with climate. For instance, the canine fossa is less marked and the frontal process of the maxilla is more anteriorly placed in populations from tropical regions; the orientation of the processus frontosphenoidalis is more forward facing. Finally, our study reveals a strong but specific relationship between atmospheric pressure and the shape of the alveolar part of the mid-face. According to the loading information, the primary factor affecting the correlation is not the maximum or minimum average pressure, but the annual range of variation between maximum and minimum values. Atmospheric pressure variation is usually measured on a short time-scale (to predict wind directions in weather-forecasting), from days to hours, while in our study we selected minimum and maximum

pressure levels at each geographic location from monthly averages. Very little information is available about monthly averages of atmospheric pressure and it is not a common parameter used to define climates; we were thus not able to connect this factor to any known, well-defined environment. However, these results should be taken with caution, for several reasons. First, the alveolar is a morphologically unstable part of the mid-face, and it is known to be affected by age and teeth conditions, among other confounding variables (Small et al., 2016). Second, the correlation is mainly driven by the North and South Chinese, who are genetically close and the only two groups enduring a wide sea-level pressure level annual variation (Fig. 1). When the analysis is rerun without these two populations, the correlation disappears in the Mantel test and SV2 of the PLS is not specifically impacted by the sea-level pressure loadings any more (data not shown), suggesting that the observed association could be a by-product of a morphological specificity of the Chinese group not related to atmospheric pressure. This point is also supported by the lack of obvious biological link between this climatic variable and alveolar shape. Clearly, further studies specifically focusing on populations originating from locations with a great diversity of atmospheric pressures will be needed to confirm or reject this correlation.

CONCLUSION

Bony surfaces provide new information on the variation in skeletal morphology. This study focuses for the first time on the association between surface morphology of the mid-face and variable climatic parameters. Furthermore, genetic data were included to correct for spurious associations caused by phylogenetic relationships between populations rather than climatic factors. Our findings confirm the previously reported association of climatic variables with facial shape, especially the nasal aperture (Coon et al., 1950; Carey and Steegmann, 1981; Roseman, 2004; Roseman and Weaver, 2004; Nicholson and Harvati, 2006), and reveal new trends, with the zygomatic becoming more prominent and the nasal aperture becoming more rectangular in populations living in temperate climates compared to populations from tropical climates. The adaptation to colder temperatures in temperate climates and to high sunshine exposure in tropical climates may have played a role in the observed differences. We also observed a surprising impact of sea-level pressure on the alveolar shape, with populations enduring larger annual variation of atmospheric pressure having deeper alveolar. Whether this correlation reflects a real biological adaptation or is a statistical artefact will deserve further investigation. Climate is one of the most important factors shaping the biodiversity on Earth, and this study has enriched our understanding on its role with regard to human diversity.

ACKNOWLEDGEMENTS

We are indebted to Dr. Xiujie Wu (IVPP) who kindly shared her skeletal scans with us. We are grateful to curators and collection managers at the IVPP (Beijing), the Evidence Identification Centre of Public Security Bureau of China's Ministry of Public Security (Beijing), the Kenya National Museum (Nairobi) and the American Museum of Natural History (New York) for providing access to their specimens. The authors also thank Dr. Melinda Yang and two anonymous reviewers who provided valuable comments to improve this paper.

LITERATURE CITED

Ackermann RR. 2005. Ontogenetic integration of the hominoid face. J Hum Evol 48:175–197.

Adams DC, Otarola-Castillo E. 2013. Geomorph: an r package for the collection and analysis of geometric morphometric shape data. Methods Ecol Evol 4:393–399.

Airey DK, Wong JCF, Fleming RA. 1995. A comparison of human- and headform-based measurements of solar ultraviolet B dose. Photodermatol Photoimmunol Photomed 11:155–158.

Beall, CM, Jablonski NG, Steegmann AT. 2012. Human adaptation to climate: temperature, ultraviolet radiation, and altitude In: Stinson S, Bogin B, O'Rourke D, editors. Human biology: an evolutionary and biocultural perspective. 2nd ed. New York: Wiley. p 175–250.

Bjornstad ON, Falck W. 2001. Nonparametric spatial covariance functions: estimation and testing. Environ Ecol Stat 8:53–70.

Blum HF. 1961. Does the melanin pigment of human skin have adaptive value: an essay in human ecology and the evolution of race. Q Rev Biol 36:50–63.

Bookstein FL. 1989. Principal warps—thin-plate splines and the decomposition of deformations. IEEE Trans Pattern Anal Mach Intell 11:567–585.

Carey JW, Steegmann AT, Jr. 1981. Human nasal protrusion, latitude, and climate. Am J Phys Anthropol 56:313–319.

Clement AF, Hillson SW, Aiello LC. 2012. Tooth wear, Neanderthal facial morphology and the anterior dental loading hypothesis. J Hum Evol 62:367–376.

Consortium HP-AS, Abdulla MA, Ahmed I, Assawamakin A, Bhak J, Brahmachari SK, Calacal GC, Chaurasia A, Chen CH, Chen J, Chen YT, Chu J, Cutiongco-de la Paz EM, De Ungria MC, Delfin FC, Edo J, Fuchareon S, Ghang H, Gojobori T, Han J, Ho SF, Hoh BP, Huang W, Inoko H, Jha P, Jinam TA, Jin L, Jung J, Kangwanpong D, Kampuansai J, Kennedy GC, Khurana P, Kim HL, Kim K, Kim S, Kim WY, Kimm K, Kimura R, Koike T, Kulawonganunchai S, Kumar V, Lai PS, Lee JY, Lee S, Liu ET, Majumder PP, Mandapati KK, Marzuki S, Mitchell W, Mukerji M, Naritomi K, Ngamphiw C, Niikawa N, Nishida N, Oh B, Oh S, Ohashi J, Oka A, Ong R, Padilla CD,, Palittapongarnpim P, Perdigon HB, Phipps ME, Png E, Sakaki Y, Salvador JM, Sandraling Y, Scaria V, Seielstad M, Sidek MR, Sinha A, Srikummool M, Sudoyo H, Sugano S, Suryadi H, Suzuki Y, Tabbada KA, Tan A, Tokunaga K, Tongsima S, Villamor LP, Wang E, Wang Y, Wang H, Wu JY, Xiao H, Xu S, Yang JO, Shugart YY, Yoo HS, Yuan W, Zhao G, Zilfalil BA, Indian Genome Variation C. 2009. Mapping human genetic diversity in Asia. Science 326: 1541–1545.

Coon, CS, Garn, SM, Birdsell JB. 1950. Races: a study of the problems of race formation in man. Springfield: Charles C. Thomas.

Downs N, Parisi A. 2009. Measurements of the anatomical distribution of erythemal ultraviolet: a study comparing exposure distribution to the site incidence of solar keratoses, basal cell carcinoma and squamous cell carcinoma. Photochem Photobiol Sci 8:1195–1201.

Evteev A, Cardini AL, Morozova I, O'Higgins P. 2014. Extreme climate, rather than population history, explains mid-facial morphology of Northern Asians. Am J Phys Anthropol 153:449–462.

Evteev AA, Movsesian AA. 2016. Testing the association between human mid-facial morphology and climate using autosomal, mitochondrial, Y chromosomal polymorphisms and cranial non-metrics. Am J Phys Anthropol 159:517–522.

Freidline SE, Gunz P, Harvati K, Hublin JJ. 2012a. Middle Pleistocene human facial morphology in an evolutionary and developmental context. J Hum Evol 63:723–740.

Freidline SE, Gunz P, Jankovic I, Harvati K, Hublin JJ. 2012b. A comprehensive morphometric analysis of the frontal and zygomatic bone of the Zuttiyeh fossil from Israel. J Hum Evol 62:225–241.

Freidline SE, Gunz P, Harvati K, Hublin JJ. 2013. Evaluating developmental shape changes in Homo antecessor subadult facial morphology. J Hum Evol 65:404–423.
Freidline SE, Gunz P, Hublin JJ. 2015. Ontogenetic and static allometry in the human face: contrasting Khoisan and Inuit. Am J Phys Anthropol 158:116–131.
Garn SM. 1965. Human races. 2nd ed. Springfield: Thomas.
Genomes Project C, Abecasis GR, Auton A, Brooks LD, DePristo MA, Durbin RM, Handsaker RE, Kang HM, Marth GT, McVean GA. 2012. An integrated map of genetic variation from 1,092 human genomes. Nature 491:56–65.
Gunz, P, 2005. Statistical and geometric reconstruction of hominid crania, reconstructing australopithecine ontogeny. Vienna: University of Vienna.
Gunz P, Bookstein FL, Mitteroecker P, Stadlmayr A, Seidler H, Weber GW. 2009a. Early modern human diversity suggests subdivided population structure and a complex out-of-Africa scenario. Proc Natl Acad Sci USA 106:6094–6098.
Gunz P, Harvati K. 2007. The Neanderthal "chignon": variation, integration, and homology. J Hum Evol 52:262–274.
Gunz P, Mitteroecker P, Neubauer S, Weber GW, Bookstein FL. 2009b. Principles for the virtual reconstruction of hominin crania. J Hum Evol 57:48–62.
Hannam AG, Wood WW. 1989. Relationships between the size and spatial morphology of human masseter and medial pterygoid muscles, the craniofacial skeleton, and jaw biomechanics. Am J Phys Anthropol 80:429–445.
Harvati K, Hublin JJ, Gunz P. 2010. Evolution of middle-late Pleistocene human cranio-facial form: a 3-D approach. J Hum Evol 59: 445–464.
Harvati K, Weaver TD. 2006. Human cranial anatomy and the differential preservation of population history and climate signatures. Anat Rec Discov Mol Cell Evol Biol 288:1225–1233.
Holm S. 1979. A simple sequentially rejective multiple test procedure. Scand J Stat 6:65–70.
Holton N, Yokley T, Butaric L. 2013. The morphological interaction between the nasal cavity and maxillary sinuses in living humans. Anat Rec Adv Integr Anat Evol Biol 296:414–426.
Holton NE, Yokley TR, Franciscus RG. 2011. Climatic adaptation and Neandertal facial evolution: a comment on Rae et al. (2011). J Hum Evol 61:624–627 (author reply 628–629).
Howells WW. 1973. Cranial variation in man: a study by multivariate analysis of patterns of difference among recent populations. Cambridge: Harvard University Press.
Howells WW. 1989. Skull shapes and the map. Peabody mus. Arch Ethnol Camb Mass: Harvard University Press.
Hubbe M, Hanihara T, Harvati K. 2009. Climate signatures in the morphological differentiation of worldwide modern human populations. Anat Rec (Hoboken) 292:1720–1733.
Jablonski NG, Chaplin G. 2000. The evolution of human skin coloration. J Hum Evol 39:57–106.
Mantel N. 1967. The detection of disease clustering and a generalized regression approach. Cancer Res 27:209–220.
Martin R. 1988. Anthropologie, Handbuch der vergleichenden Biologie des Menschen. Stuttgart: Gustav Fisher Verlag.
Nicholson E, Harvati K. 2006. Quantitative analysis of human mandibular shape using three-dimensional geometric morphometrics. Am J Phys Anthropol 131:368–383.
Noback ML, Harvati K. 2015. The contribution of subsistence to global human cranial variation. J Hum Evol 80:34–50.
Noback ML, Harvati K, Spoor F. 2011. Climate-related variation of the human nasal cavity. Am J Phys Anthropol 145:599–614.
Pan L, Wei D, Wu XJ. 2014. Latitudinal and climatic distributions of 3D craniofacial features among Holocene populations. Sci China Earth Sci 57:1692–1700.
Pope GG. 1991. Evolution of the zygomaticomaxillary region in the genus homo and its relevance to the origin of modern humans. J Human Evol 21:189–213.
Powell JF, Neves WA. 1999. Craniofacial morphology of the first Americans: pattern and process in the peopling of the new world. Yearb Phys Anthropol 42:153–188.
R_Developmen_Core_Team. 2013. R, a language and environment for statistical computing. Vienna.
Relethford JH. 2009. Race and global patterns of phenotypic variation. Am J Phys Anthropol 139:16–22.
Relethford JH. 2010. Population-specific deviations of global human craniometric variation from a neutral mode. Am J Phys Anthropol 142.
Rohlf FJ, Corti M. 2000. Use of two-block partial least-squares to study covariation in shape. Syst Biol 49:740–753.
Rohrich RJ, Pessa JE. 2007. The fat compartments of the face: anatomy and clinical implications for cosmetic surgery. Plast Reconstr Surg 119:2219–2227; discussion 2228–2231.
Roseman CC. 2004. Detecting interregionally diversifying natural selection on modern human cranial form by using matched molecular and morphometric data. Proc Natl Acad Sci USA 101:12824–12829.
Roseman CC, Weaver TD. 2004. Multivariate apportionment of global human craniometric diversity. Am J Phys Anthropol 125: 257–263.
Rossell-Perry P. 2013. The zygomatic ligament of the face: a critical review. OA Anat 11:3.
Shea BT. 1977. Eskimo craniofacial morphology, cold stress and the maxillary sinus. Am J Phys Anthropol 47:289–300.
Small C, Brits D, Hemingway J. 2016. Assessing the effects of tooth loss in adult crania using geometric morphometrics. Int J Legal Med 130:233–243.
Smith HF. 2011. The role of genetic drift in shaping modern human cranial evolution: a test using microevolutionary modeling. Int J Evol Biol 2011:145262.
Steegmann AT, Jr. 1970. Cold adaptation and the human face. Am J Phys Anthropol 32:243–250.
von Cramon-Taubadel N. 2009. Revisiting the homoiology hypothesis: the impact of phenotypic plasticity on the reconstruction of human population history from craniometric data. J Hum Evol 57:179–190.
Weaver TD, Roseman CC, Stringer CB. 2007. Were Neandertal and modern human cranial differences produced by natural selection or genetic drift? J Human Evol 53:135–145.
Witzel U, Preuschoft H. 2002. Function-dependent shape characteristics of the human skull. Anthropol Anz 60:113–135.